RESEARCH PAPER

Dissecting the genetic control of natural variation in sorghum photosynthetic response to drought stress

Diego Ortiz[1,2], [ID] **and Maria G. Salas-Fernandez**[1,*], [ID]

[1] Department of Agronomy, Iowa State University, Ames, IA 50011, USA
[2] Instituto Nacional de Tecnologia Agropecuaria, Manfredi, Cordoba 5988, Argentina.

* Correspondence: mgsalas@iastate.edu

Abstract

Drought stress causes crop yield losses worldwide. Sorghum is a C_4 species tolerant to moderate drought stress, and its extensive natural variation for photosynthetic traits under water-limiting conditions can be exploited for developing cultivars with enhanced stress tolerance. The objective of this study was to discover genes/genomic regions that control the sorghum photosynthetic capacity under pre-anthesis water-limiting conditions. We performed a genome-wide association study for seven photosynthetic gas exchange and chlorophyll fluorescence traits during three periods of contrasting soil volumetric water content (VWC): control (30% VWC), drought (15% VWC), and recovery (30% VWC). Water stress was imposed with an automated irrigation system that generated a controlled dry-down period for all plants, to perform an unbiased genotypic comparison. A total of 60 genomic regions were associated with natural variation in one or more photosynthetic traits in a particular treatment or with derived variables. We identified 33 promising candidate genes with predicted functions related to stress signaling, oxidative stress protection, hormonal response to stress, and dehydration protection. Our results provide new knowledge about the natural variation and genetic control of sorghum photosynthetic response to drought with the ultimate goal of improving its adaptation and productivity under water stress scenarios.

Keywords: Chlorophyll fluorescence, drought, genome-wide association study, natural variation, photosynthesis, sorghum.

Introduction

Drought is a major abiotic stress that causes substantial yield losses worldwide (Li *et al.*, 2009). The large environmental variability associated with climate change may intensify future abiotic stress events (FAO, 2016), and this could lead to increased risks of food shortages, especially in regions with fast-growing populations.

Tropical C_4 cereals such as maize (*Zea mays*) and sorghum (*Sorghum bicolor* L.) present a relative advantage in water–use efficiency over C_3 crops in temperate regions. The anatomical and biochemical characteristics associated with the CO_2–concentrating mechanism in C_4 species allow plants to reach high net assimilation rates (*A*) at low stomatal conductance (g_s) levels (Long, 1999; Taylor *et al.*, 2010). Sorghum can tolerate moderate drought conditions due to its deep root system that can extract water from dry soils and thus sustain stomatal opening at low water potential. Further, some sorghum accessions have leaf wax that reflects excess light and

reduces cuticular conductance (Tari *et al.*, 2013). However, under a more severe water shortage, both growth and yield are reduced due to a negative effect on cell expansion, *A*, and partitioning of assimilates to harvestable organs (Peng *et al.*, 1991; Sankarapandian *et al.*, 2013).

The effects of drought on photosynthesis can be divided into stomatal and non-stomatal processes (Lawlor, 2002). As water limitation in the soil progresses, plants tend to close stomata, and thus g_s and transpiration (*E*) are reduced, limiting *A*. However, under more severe water stress, non-stomatal processes are also affected, resulting in a reduction of both leaf photochemistry and carbon metabolism, and an increase in oxidative stress (Chaves *et al.*, 2009).

A combination of drought and high light intensity generates an excess of energy that can lead to photoinhibition—the inactivation of PSII activity. Under these circumstances, photoprotection mechanisms play a key role in preventing damage to the photosynthetic machinery. Plants can dissipate excess light energy as heat through conformational changes in the light-harvesting complex (LHC). The process is mediated by the xanthophyll cycle, which consists of the de-epoxidation of violaxanthin to zeaxanthin in response to high light intensity, providing a mechanism to prevent photoinhibition and minimize oxidative stress (Demmig-Adams *et al.*, 1989; Ruban *et al.*, 2012). Changes in the efficiency of light reactions and the level of photosystem damage can be assessed using pulse amplitude modulation (PAM) fluorometers. Chlorophyll fluorescence variables have been successfully used in studies of cold, salinity, heat, and drought stresses, and the information gained can help to discover genotypic variation associated with drought tolerance (Netondo *et al.*, 2004; Hund *et al.*, 2005; Kościelniak *et al.*, 2005; Kiani *et al.*, 2008; Ortiz *et al.*, 2017).

Selection for higher photosynthetic performance has been proposed as a feasible goal for increasing crop yields (Long *et al.*, 2006; Flood *et al.*, 2011). There is extensive natural variation in *A* and the ratio between *A* and *E* (*A*:*E*) in sorghum under both non-stress and abiotic stress conditions (Kidambi *et al.*, 1990b; Peng *et al.*, 1991; Balota *et al.*, 2008; Xin *et al.*, 2009; Salas Fernandez *et al.*, 2015; Ortiz *et al.*, 2017). While variation in *A* and *A*:*E* suggests that selection for higher carbon fixation is possible, the genetic architecture of photosynthetic processes under drought stress has not been unraveled in sorghum. The objective of this study was to discover the markers/genomic regions and candidate genes associated with natural variation in gas exchange and chlorophyll fluorescence traits under well-irrigated and water-limited conditions. Our findings can be leveraged in breeding programs and exploited in engineering/editing efforts to develop superior germplasm adapted to drought-prone environments.

Materials and methods

Germplasm

A total of 324 accessions from the Sorghum Association Panel (SAP) that captures the worldwide natural variation in photosynthetic capacity within the species were used herein (Casa *et al.*, 2008). The SAP has been used in quantitative genetic studies to investigate numerous traits including photosynthetic response to cold stress (Sukumaran *et al.*, 2012, Morris *et al.*, 2013; Mantilla Perez *et al.*, 2014; Zhao *et al.*, 2016; Ortiz *et al.*, 2017).

Experimental design

Accessions were evaluated in an incomplete block design, consisting of nine incomplete blocks (sets) and two replicates (biological and growth chamber variation). Each set was composed of plants representing 40 accessions and augmented with the following checks: PI656029 (B35), PI655996 (Tx430), PI533839 (Camjin), and PI564163 (BTx623). These checks were selected based on preliminary measurements of *A* under drought stress. PI564163 and PI533839 are contrasting accessions for photosynthetic capacity, while PI655996 and PI656029 are known for their drought tolerance during vegetative and reproductive stages, respectively (Sanchez *et al.*, 2002; Balota *et al.*, 2008).

Growth conditions

In each set, 18 seeds per accession were planted in seedling trays and grown in a greenhouse for 12 d. Subsequently, two plantlets per accession were transplanted into 6 liter pots, filled with Metro Mix 900 soil (Sungro Horticulture), and one plant per accession was assigned to each of the two growth chambers equipped with metal halide and high-pressure sodium lamps (Percival, model PGW36T, capacity 11.28 m³). Plants were gradually adapted to high-light conditions during the first 2 weeks—from 400 µmol photons m^{-2} s^{-1} to 1000 µmol photons m^{-2} s^{-1}. Growing conditions in growth chambers were 28 °C day 24 °C night, 16 h photoperiod, 1000 µmol photons m^{-2} s^{-1}, and 40–60% relative humidity. Each day, light intensity was increased and decreased during the first and last 2 h of the 16 h period to simulate sunrise and sunset. Fertilization was applied as needed until the start of the water treatments with 130 ppm N of Peters Excel Cal-Mag Fertilizer (15-5-5).

Soil water content was controlled in individual pots using a customized automated irrigation system described in Ortiz *et al.* (2018). Briefly, the system was based on the use of capacitance sensors in each pot, a multiplexer AM16/32B (Campbell Scientific, Logan, UT, USA), a data logger CR1000 (Campbell Scientific), and a microcontroller Mega 2560 (Arduino, Ivrea, Italy) acting as a relay driver to trigger irrigation of specific pots, if needed, to achieve the desirable volumetric water content (VWC) (Fig. 1A, B). Plants were subjected to three consecutive water treatments 30 d after planting: control or non-stress for 3 d at >30% VWC; drought that included 7 d of constant dry-down and 3 d at 15% VWC; and recovery for 5 d, when plants were re-watered and maintained at >30% VWC (Fig. 1C).

Photosynthesis and chlorophyll fluorescence

Gas exchange and chlorophyll fluorescence measurements were collected using three LI-COR 6400 XT portable gas analyzers equipped with 6400-40 Leaf Chamber Fluorometer (LI-COR, Lincoln, NE, USA). Measurements were taken on days 1–3 of control, 8–10 of drought, and 2 and 5 of the recovery treatment (Fig. 1C). The youngest fully expanded leaf was selected for measurements during the control period, and a new leaf identified according to the same criterion was used during the drought and recovery treatments to prevent aging effects.

Dark-adapted fluorescence measurements were taken at 07.00 h. Maximum quantum yield of PSII (F_v/F_m) was recorded in an overnight dark-adapted leaf using an aluminum foil cover. A modulating radiation of three was used to obtain minimum chlorophyll fluorescence (F_0), and a flash of 8000 µmol m^{-2} s^{-1} was applied for 3 s to record maximum chlorophyll fluorescence (F_m). Results were used to calculate variable chlorophyll fluorescence (F_v), as $F_m - F_0$, and maximum quantum yield of PSII as F_v/F_m.
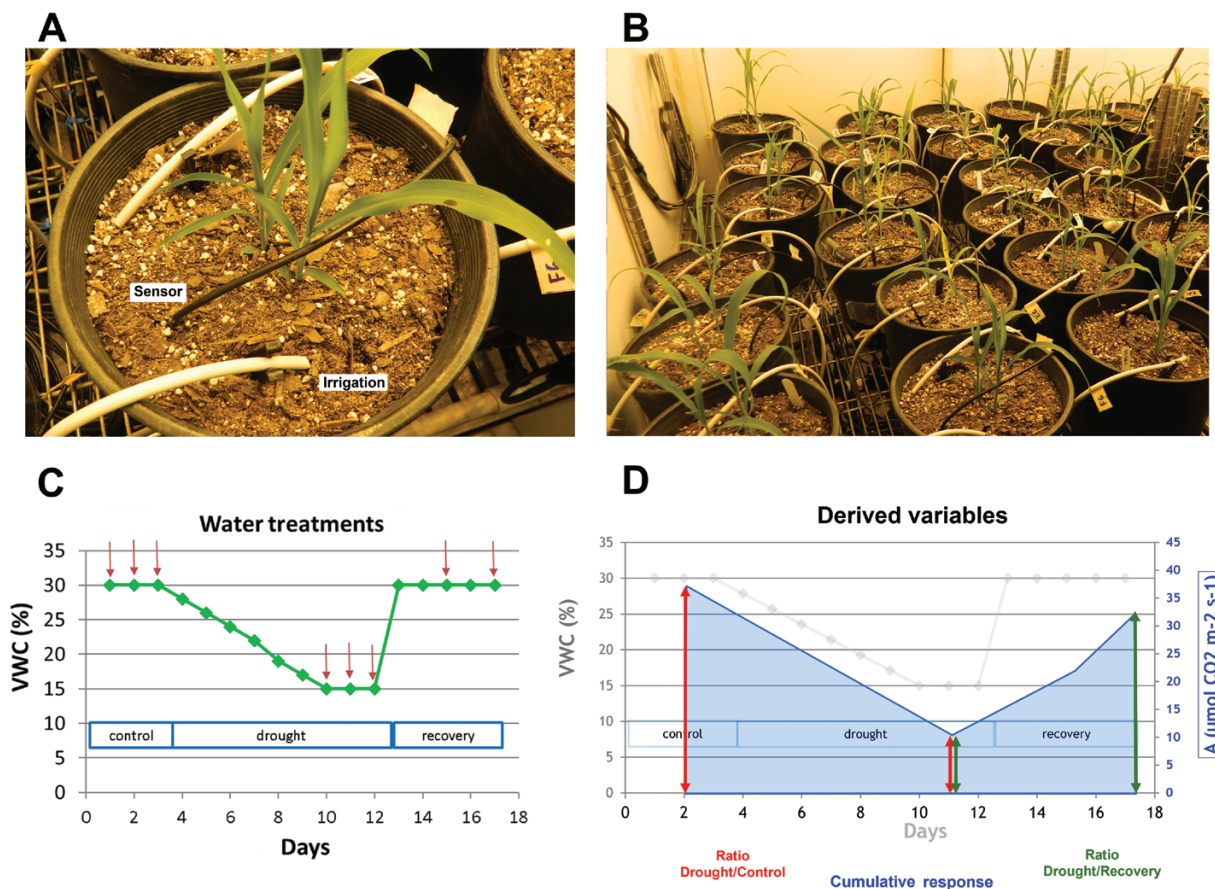
Fig. 1. Irrigation system and treatments imposed to induce drought stress. (A) Close-up view of the irrigation and water sensor in an individual pot. (B) Arrangement of the irrigation system in growth chambers. (C) Volumetric water content (VWC) and duration of control, drought, and recovery treatments. Arrows indicate time points of photosynthesis and chlorophyll fluorescence measurements. (D) Graphical representation of the derived variables 'cumulative response', 'ratio drought–control', and 'ratio drought–recovery'.

After a minimum of 30 min of exposure to high-light conditions, gas exchange and light-adapted chlorophyll fluorescence parameters were measured between 09.00 h and 14.00 h in the same leaf used for dark-adapted fluorescence. Conditions in the LI-COR 6400XT leaf chamber cuvette were set to 1000 μmol photons m^{-2} s^{-1} photosynthetically active radiation (PAR), 400 ppm reference CO_2 concentration, and 50–60% relative humidity. Leaf temperature was set to 28 °C during control and recovery days but was not controlled during the drought treatment in order to capture genotypic differences in leaf temperature regulation under stress. The fraction of blue light was 10% of the PAR level to maximize stomatal aperture. Light-adapted minimum chlorophyll fluorescence (F_0') and maximum chlorophyll fluorescence (F_m') were determined using a measuring light intensity of three and a saturating pulse of 8000 μmol photons m^{-2} s^{-1} for 0.8 s, respectively. Plants were allowed to stabilize for a minimum of 2 min, and subsequently four parameters were monitored for stability: A, g_s, steady-state fluorescence, and water vapor concentration. Data were recorded when the four parameters were stable, and the overall coefficient of variation was <1.2%. The following gas exchange parameters were obtained: A, g_s, and E. Chlorophyll fluorescence parameters included effective quantum yield of PSII (Φ_{PSII}), efficiency of energy captured by open PSII reaction centers (F_v'/F_m'), and fraction of reaction centers that are open (qP) (Genty *et al.*, 1989; Maxwell and Johnson, 2000). Additionally, the ratio between A and E was calculated (A:E). This variable is used to detect differences in transpired water use efficiency.

Three derived variables for each photosynthetic trait were calculated to dissect the genotypic response over water treatments: (i) 'cumulative response' (area underneath the curve); (ii) the ratio between drought and control; and (iii) the ratio between drought and recovery (Fig. 1D). Cumulative response variables capture the overall response to the three water treatments, while ratios characterize the genotypic response to a particular treatment relative to its maximum (ratio of drought to control) or minimum (ratio of drought to recovery) values. Thus, ratio variables can provide information about the relative sensitivity of genotypes to drought and recovery.

Statistical analysis

All variables were analyzed per water treatment using each day within a treatment as a repeated measure. Response variables were modeled using a linear mixed model and evaluated with SAS version 9.4 (SAS Institute, Cary, NC, USA). Selection of the best model was performed by comparing the Akaike information criterion (AIC) and Bayesian information criterion (BIC) of models with alternative combinations of covariates, namely leaf temperature, vapor pressure deficit, and SWC.

For A, E, g_s, F_v'/F_m', Φ_{PSII}, and qP in control, the model was:

$$Y_{ijklm} = \mu + S_i + R_{(i)j} + D_k + G_l + M_m + \varepsilon_{ijklm} \quad (1)$$

where Y_{ijklm} is the response variable, μ is the intercept, S_i is the set (incomplete block) effect, $R_{(i)j}$ is the replication nested in set effect (growth

chamber), D_k is the day effect, G_l is the accession (genotypic) effect, M_m represents machine (gas analyzer) effects, and ε_{ijklm} is the residual.

For A, E, g_s, F_v'/F_m', Φ_{PSII}, and qP in drought and recovery, the model was:

$$Y_{ijklmn} = \mu + S_i + R_{(i)j} + D_k + G_l + M_m + T_n + \varepsilon_{ijklmn} \quad (2)$$

where T_n is leaf temperature effect.

For F_v/F_m in control, drought, and recovery, the model was:

$$Y_{ijkl} = \mu + S_i + R_{(i)j} + D_k + G_l + \varepsilon_{ijkl} \quad (3)$$

In all models, day, leaf temperature, and machine were considered fixed effects, while set, replication nested in set, and accession effects were considered random. For each variable, values scaled to corresponding units were obtained based on best linear unbiased predictions (BLUPs) and used as phenotypes in the genome-wide association study (GWAS). The information for descriptive statistics including estimates of correlation coefficients were generated with PROC CORR in SAS 9.4.

The intraclass correlation (h^2) was estimated as:

$$h^2 = \sigma^2_G / [\sigma^2_G + (\sigma^2_\varepsilon / r)]$$

where σ^{22}_G is the estimate of accession variance, σ^2_ε is the estimate of error variance, and r is the number of replications. The intraclass correlation, as estimated herein, provides an estimate of repeatability.

GWAS

A publicly available set of ~ 260 000 single nucleotide polymorphisms (SNPs) (http://www.morrislab.org/data) obtained with genotyping-by-sequencing technology (Elshire *et al.*, 2011) were utilized after filtering for <40% of missing data and minimum allele frequency of 5%. A final set of 134 200 markers were retained for the analysis.

A mixed linear model was fitted using Tassel 5.12, accounting for population structure (Q, fixed) and kinship (K, random) to minimize spurious associations (Zhang *et al.*, 2010). Q matrix, which accounts for the effects of a structured population, was estimated using STRUCTURE 2.2.3 (Pritchard *et al.*, 2000), and K matrix, which accounts for the degree of relatedness among accessions, was estimated using SPAGeDi (Hardy and Vekemans, 2002), as reported in Mantilla Perez *et al.* (2014). QVALUE software was used to calculate false discovery rates, to control for false positive associations due to multiple comparisons (Storey and Tibshirani, 2003).

Co-localization of associated markers with known quantitative trait loci (QTL) controlling drought response or photosynthesis-related traits

QTL physical coordinates and target traits were extracted from the Sorghum QTL Atlas (Mace *et al.*, 2019) for the following 17 studies investigating drought stress response and/or photosynthesis-related traits in sorghum: (i) stay-green under field drought stress (Crasta *et al.*, 1999; Subudhi *et al.*, 2000; Tao *et al.*, 2000; Xu *et al.*, 2000; Haussmann *et al.*, 2002; Srinivas *et al.*, 2009); (ii) carbon assimilation and transpiration for pre-flowering drought applied in a greenhouse setting (Kapanigowda *et al.*, 2014); (iii) stay-green and pre-flowering tolerance under field drought conditions (Kebede *et al.*, 2001); (iv) gas exchange and/or chlorophyll fluorescence under temperature stress in controlled environments (Fiedler *et al.*, 2014, 2016; Ortiz *et al.*, 2017); (v) grain yield, morphology, and plant architecture under pre-flowering drought conditions in field experiments (Phuong *et al.*, 2013); (vi) chlorophyll content and biomass under cold and heat stress (Chopra *et al.*, 2017); (vii) stay-green and grain yield under field drought conditions (Sabadin *et al.*, 2012; Rama Reddy *et al.*, 2014); (viii) leaf drying rate under drought imposed in a greenhouse setting (Sakhi *et al.*, 2013); and (ix) stay-green, agronomic traits,

chlorophyll content, and chlorophyll fluorescence under drought in field trials (Sukumaran *et al.*, 2016). The co-localization of significant markers with these published QTL was investigated using the Sorghum genome v3 physical coordinates.

Identification of candidate genes in significantly associated regions

Linkage disequilibrium (LD) regions were defined as in Ortiz *et al.* (2017). Candidate genes within 55 kb from significant markers were identified using the Sorghum genome v3. Of this comprehensive list, the most promising candidates were selected based on the following criteria: (i) their expression in leaves according to 48 microarray and RNAseq experiments (McCormick *et al.*, 2018); (ii) their differential expression under pre-flowering drought conditions based on a transcriptome field study of elite inbred lines BTx642 (post-flowering drought tolerant) and RTx430 (pre-flowering drought tolerant) (Varoquaux *et al.*, 2019); and/or (iii) predicted peptide signal targeting the encoded protein to the chloroplast or mitochondria according to TargetP-2.0 (Almagro Armenteros *et al.*, 2019). This reduced list of suggested genes for future validation studies was further reduced based on their predicted functions and homology to genes with a potential role in drought stress response and carbon fixation.

Results

Analysis of phenotypes

Our automated irrigation system provided the ability to control the dry-down of potted plants during a 7 d period and was able to maintain a final VWC of 15±5% (Supplementary Table S1). This precise soil water control is comparable with those attained with large-scale automated phenotyping platforms (Granier *et al.*, 2006; Finkel, 2009; Junker *et al.*, 2015).

Water treatments affected all photosynthetic parameters, as expected, with the largest among-treatment differences observed between control and drought, followed by differences between control and recovery (Fig. 2). In general, relative differences attributed to drought were greater for gas exchange variables (52–61%) than for chlorophyll fluorescence traits (3–44%). Stomatal conductance was the most drastically reduced parameter during the drought period in all genotypes, while F_v/F_m and $A{:}E$ had the minimum response to stress (2% reduction).

There were multiple significant estimates of correlation among traits within treatments (Supplementary Tables S2–S4). Gas exchange variables were highly correlated with each other, and A was consistently correlated with Φ_{PSII} in all water treatments (Supplementary Table S2; Supplementary Figs S1, S2). Even though qP and F_v'/F_m' were both highly correlated with Φ_{PSII}, the correlation between the two former variables was low to intermediate within water treatments ($r=0.19$–0.61) (Supplementary Tables S2–S4). In general, F_v/F_m presented low or no correlation with most variables under non-stress (Supplementary Table S2), but those associations increased under drought (Supplementary Tables S3, S4).
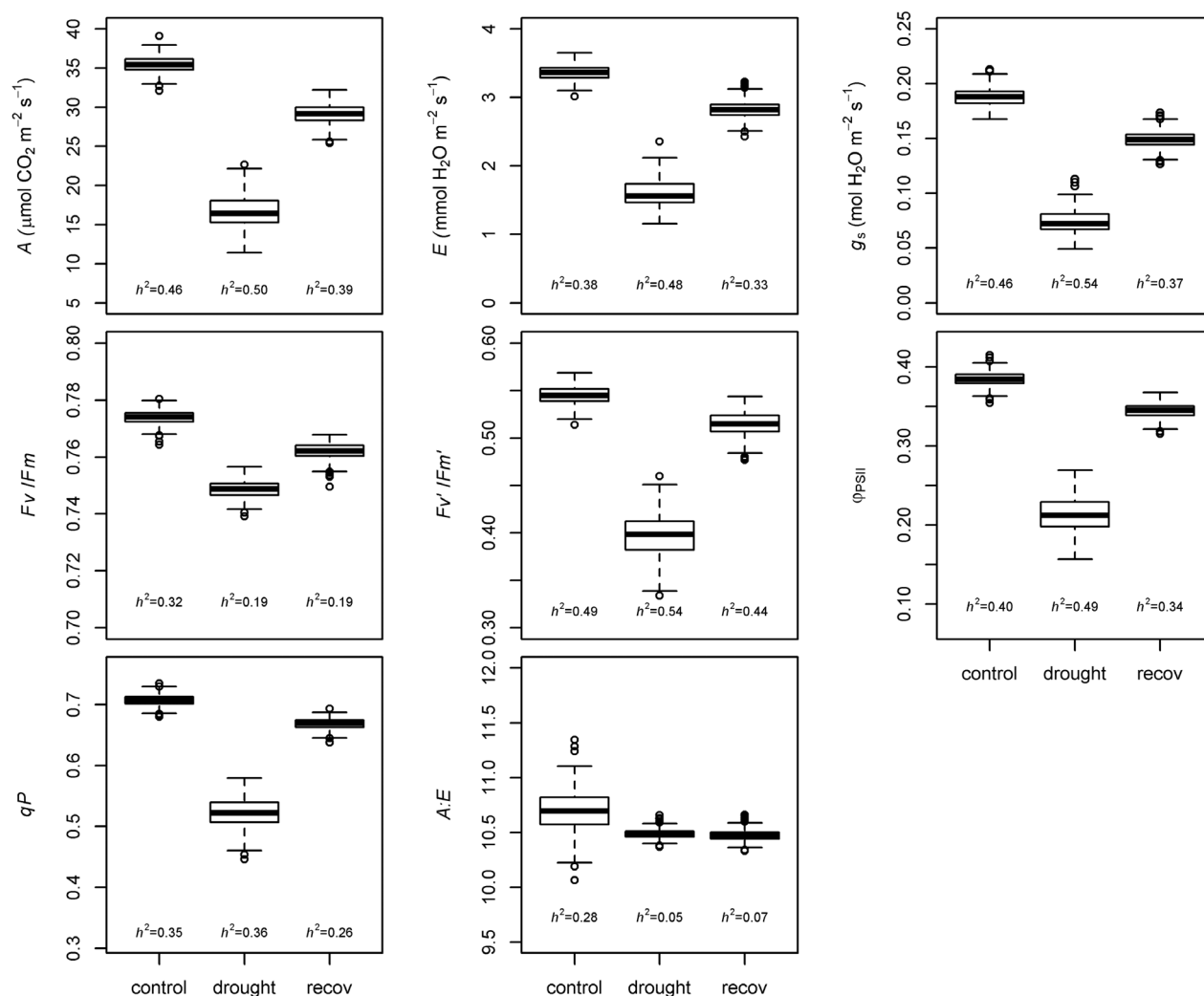
Fig. 2. Box plots of gas exchange and chlorophyll fluorescence traits based on BLUPs for control, drought, and recovery periods. h^2, heritability; *A*, photosynthesis; *E*, transpiration, g_s, stomatal conductance, F_v/F_m, maximum quantum yield of PSII, Φ_{PSII}, effective quantum yield of PSII; F_v'/F_m', efficiency of energy captured by open PSII reaction centers; qP, photochemical quenching or fraction of PSII reaction centers that are open, and *A:E*, ratio between photosynthesis and transpiration.

The ANOVA confirmed that genotypes from the SAP exhibit significant variation in all traits and water treatments, except for *A:E* during drought and recovery periods (Supplementary Table S5). Among the fixed effect factors, T_{leaf} was significant for most variables except g_s in recovery, while machine was not significant for F_v'/F_m' during the same period. In general, estimates of repeatability were intermediate (0.26–0.54), but low for F_v/F_m and *A:E* during the drought and recovery periods, ranging from 0.05 to 0.19 (Fig. 2).

Genome-wide association results

Sixty regions defined by LD (labeled as chromosome#_region#) were significantly associated with seven photosynthetic traits throughout three water treatments and derived variables

(Table 1; Supplementary Table S6; Supplementary Figs S3–S10). Of the total 181 SNP–trait correlations, the majority (88%) corresponded to the recovery treatment, while only small percetanges occurred during drought, control (non-stress), or as a cumulative response (Table 1; Fig. 3). Even though there were no markers consistently associated with the same variable in different water treatments, there were cases in which regions in LD were significant for a particular trait–treatment, and its derived variable. For example, *S5_42764230* was significant for *E* control and *E* cumulative response. GWA signals were detected in all chromosomes except chromosome 9 and included a variable number of SNPs (1–31) for a single trait (Fig. 3). The percentage of phenotypic variation explained by a marker ranged from 5% to 12% (Table 1). The associated LD regions harbor a total of 796 genes located within 55 kb from the significant SNPs

Table 1. Summary of regions significantly associated with variation in photosynthesis and chlorophyll fluorescence traits during three water treatments

Trait	FDR threshold[a]	Corresponding *P*-value[b]	Chromosome	R^2 range	No. of significant LD regions
A control	0.073	5.62E-07	1	0.09–0.09	1
A recovery	0.132	5.64E-05	1,4,5,7,8,10	(0.051–0.104)	24
A cumulative response	0.05	4.50E-07	4	0.09–0.09	1
E drought	0.155	5.36E-06	4,5	0.077–0.111	3
E recovery	0.13	2.03E-05	1,2,4,5,8,10	0.06–0.115	12
E cumulative response	0.119	5.32E-06	2,4,5	0.077–0.105	5
g_s recovery	0.087	4.12E-05	1,2,3,4,5,7,8,10	0.055–0.128	31
F_v'/F_m' recovery	0.059	9.45E-06	1,2,4,5,7	0.064–0.128	10
F_v'/F_m' ratio DC	0.111	9.36E-07	4	0.11–0.11	1
F_v'/F_m' cumulative response	0.184	4.98E-06	1,5	0.074–0.095	3
Φ_{PSII} ratio DC	0.157	1.28E-06	4	0.108–0.108	1
Φ_{PSII} recovery	0.127	1.95E-035	1,4	0.059–0.104	6
qP control	0.177	1.30E-05	1,4,6,10	0.066–0.089	7
A:E recovery	0.116	1.73E-06	10	0.08–0.08	1

DC, drought–control.

[a] *P*-value corresponds to significance level of the region–trait association.

[b] False discovery rate (FDR) threshold for each trait in the GWAS. FDR was calculated, according to Storey and Tibshirani (2003), to control for false-positive associations due to multiple comparisons.
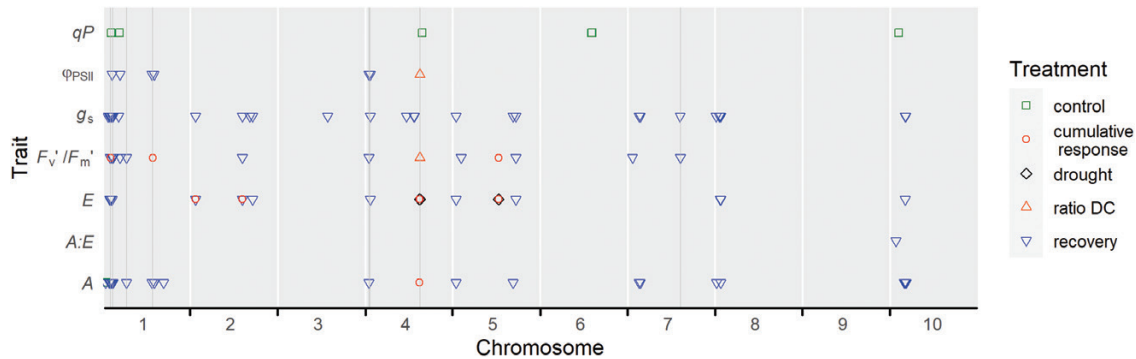

Fig. 3. Summary of genome-wide associations for photosynthesis and chlorophyll fluorescence using 324 diverse sorghum accessions. Only significant SNPs/regions are represented by a dot. *A*, photosynthesis (μmol CO_2 m^{-2} s^{-1}); *E*, transpiration rate (mmol H_2O m^{-2} s^{-1}); g_s, stomatal conductance (mol H_2O m^{-2} s^{-1}); F_v'/F_m', efficiency of energy captured by open PSII reaction centers; Φ_{PSII}, effective quantum yield of PSII; qP, photochemical quenching or fraction of PSII reaction centers that are open; and *A:E* ratio between photosynthesis and transpiration. Vertical blue lines highlight genomic regions associated with multiple traits and/or treatments.

(Supplementary Table S7). This list includes genes with predicted functions related to membrane transporters, transcription factors, oxidative stress, protein kinases, and peroxidases, among others (Supplementary Table S7, S8).

To prioritize discoveries, regions were initially grouped based on their co-localization with previously reported QTL controlling either diverse yield/agronomic characteristics under drought or photosynthesis–related traits. Out of the 60 significant LD regions, 55 overlapped with known QTL, providing independent support for the newly characterized natural variation in sorghum photosynthetic capacity (Fig. 4; Table 2; Supplementary Table S8). The remaining five regions represent novel loci that contain 13 genes differentially expressed under

pre-flowering drought stress (Fig. 4; Table 3; Supplementary Table S7, S8) (Varoquaux *et al.*, 2019). The coincident association with gas exchange and chlorophyll fluorescence parameters was the subsequent criterion used to select nine out of the 55 regions. Those nine chromosomal intervals harbor 173 predicted genes whose expression levels in response to pre-flowering drought were extracted from the RNAseq study conducted by Varoquaux *et al.* (2019). Of the 57 differentially expressed genes (Supplementary Table S9), 20 had predicted functions related to drought stress response or carbon fixation based on homology with Arabidopsis, maize, or rice genes, and 10 of them had a predicted chloroplast or mitochodria targeting sequence as determined by TargetP (Table 2).
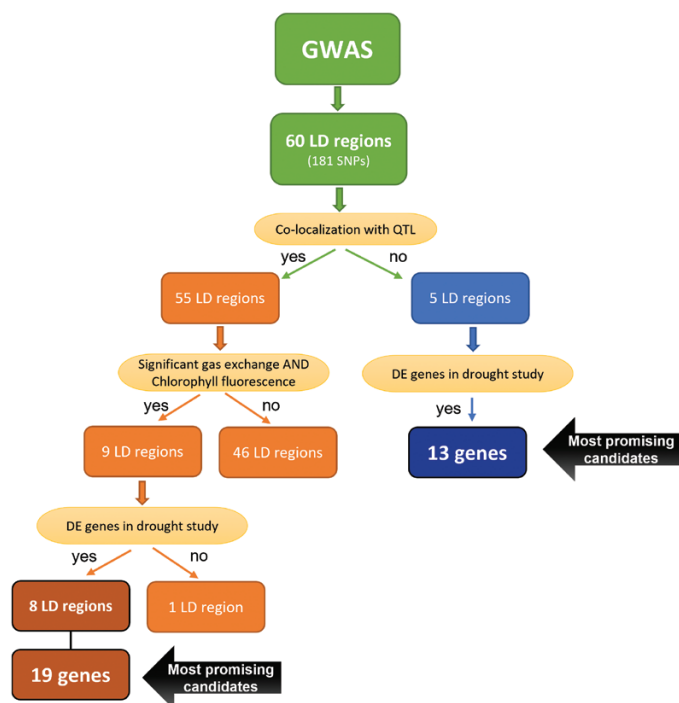
Fig. 4. Flow chart of comparative analyses conducted to identify the most promising candidate genes within significantly associated LD regions. DE, differentially expressed genes based on RNAseq study conducted under drought stress by Varoquaux *et al.* (2019).

Discussion

Most sorghum studies dissecting the genetic control of drought tolerance have focused on post-flowering stages and the effect of the stay-green trait on grain yield. Stay-green lines delay senescence and sustain leaf function for a longer period, which generates higher yields under post-anthesis drought stress (Borrell *et al.*, 2000). Leaf senescence is a programmed process that can be hastened under environmental stress (Noodén *et al.*, 1997). In our study, drought was imposed pre-flowering (8–12 expanded leaves) to investigate a less characterized phenological stage, but the identification of 43 SNPs that are located within previously reported QTL for post-flowering stay-green supports the idea that common QTL could control drought responses across phenological stages, as previously demonstrated (Burke *et al.*, 2013) (Supplementary Table S8).

In quantitative genetic studies of drought stress response, it is particularly important to impose growing conditions that will ensure consistent growth rates and phenological states for the unbiased comparison of genotypes (Collins *et al.*, 2008). Similarly, the rate of progression and duration of the drought event must be homogenously applied across genotypes since they determine the type of stress response (Mcdonald and Davies, 1996). The automated irrigation system utilized in this study and the dry-down method imposed to reach the target drought level were effective to provide water stress to all plants, increasing the chances of identifying loci associated with

drought tolerance, as suggested by Collins *et al.* (2008) and Blum (2011). Preliminary experiments conducted on a subset of lines (data not shown) demonstrated that 15% VWC was a target level that maximized the differential photosynthetic response of genotypes without inducing irreversible senescence that would have eliminated genotypes from the GWAS. Due to the broad genetic diversity of the SAP, it is possible that some genotypes (drought tolerant) experienced a moderate stress at the final VWC (15%), while others (more susceptible) suffered a severe stress at the same level. Therefore, the observed decrease in photosynthesis could be mostly due to stomatal limitations for some accessions but caused by photodamage in others.

The large range of variation in gas exchange and chlorophyll fluorescence variables observed in our study is in agreement with previous reports in sorghum (Kidambi *et al.*, 1990a; Peng *et al.*, 1991; Balota *et al.*, 2008; Guo *et al.*, 2008; Kiani *et al.*, 2008; Xin *et al.*, 2009; Salas Fernandez *et al.*, 2015; Sukumaran *et al.*, 2016; Ortiz *et al.*, 2017). The intermediate h^2 of *A*, *E*, and g_s are similar to those described by other groups (Hervé *et al.*, 2001; Gu *et al.*, 2012; Ortiz *et al.*, 2017), and suggest that selection for genotypes with higher carbon fixation capacity is possible. The decline in *A* under drought stress was coupled with proportional reductions in g_s and *E*, which implies that genotypic differences in photosynthetic performance are mostly associated with stomatal closure, as noted by Cornic (2017). Genotypic effects for *A*:*E* were not significant during the drought and recovery treatments, with narrower phenotypic variation than previously reported (Fig. 2) (Balota *et al.*, 2008). The non-stress F_v/F_m values are as expected for a C_4 species (Björkman and Demmig, 1987; Fracheboud *et al.*, 1999; Cousins *et al.*, 2002) and the decline under drought and recovery treatments is indicative of the typical photoinhibition of stressed plants. The reduction in Φ_{PSII} during drought and recovery can be explained by decreases in both energy capture (F_v'/F_m') and the fraction of open reaction centers (qP). The variability in the ratio of control to drought for F_v'/F_m' suggests that genotypes had large differences in non-photochemical quenching (NPQ) capacity, as expected (Zegada-Lizarazu and Monti, 2013), which could be exploited for the development of drought-tolerant germplasm.

Regions co-localizing with previously reported drought response or photosynthesis-related QTL

The large number of significant SNPs/genomic regions explaining small percetanges of the phenotypic variation (R^2) are consistent with the complex genetic architecture of photosynthetic traits (Table 1), which has been described in other gas exchange and chlorophyll fluorescence studies under non-stress and abiotic stress (Fracheboud *et al.*, 2002; Hao *et al.*, 2012; Strigens *et al.*, 2013; van Rooijen *et al.*, 2015), including sorghum in response to cold (Fiedler *et al.*, 2014; Ortiz *et al.*, 2017). Therefore, we prioritized discoveries based on the coincident

Table 2. Subset of significant genome-wide associations for both gas exchange and chlorophyll fluorescence traits that co-localized with known QTL for agronomic traits under drought- or photosynthesis-related parameters

GWAS Region[b]	Physical interval[c]	No. of SNPs	No. of genes[d]	Traits[d]	Overlapping QTL[a] QTL ID	Traits	Promising candidate genes ID	Predicted function	Signal[e]	DE drought[f]
1_8	7959919	1	12	A recov, g_s recov, F_v'/F_m' recov	QCHLC1.27, QCHLC1.3, QDMGR1.22, QGLFA1.1	Chlorophyll content, Dry matter growth rate, Green leaf area	Sobic.001G103300	ER-type calcium-transporting ATPase		Tx430
1_15	9983041–11205226	5	34	A recov, g_s recov, E recov, F_v'/F_m' recov, ΦPSII recov	QCHLC1.27, QCHLC1.3, QCO2A1.1, QDMGR1.2, QDMGR1.22, QGLFA1.4, QTNGL1.2, QTNGL1.3	Chlorophyll content, CO_2 assimilation ratio, Dry matter growth rate, Green leaf area, Total no. of green leaves	Sobic.001G126500, Sobic.001G127500, Sobic.001G128600, Sobic.001G129700, Sobic.001G140400, Sobic.001G140700	RNA helicase, Chaperone ABC1 prot kinase, Unknown function, germin-like protein 4, EPF-like, Pyruvate kinase family protein	Mt, Chl, Chl	Tx642, Both, Tx642, Both, Tx642, Tx430
1_19	26573871	1	6	A recov, F_v'/F_m' recov	QCHLF1.31, QDMGR1.22, QGLFA1.5, QGLFA1.6, QLFTE1.1, QLFTE1.2, QPSII1.42, QPSII1.43, QPSII1.44, QSTCD1.24, QTRSP1.2, QWUEF1.1	Chlorophyll fluorescence, Dry matter growth rate, Green leaf area, Transpiration rate, Effective quantum yield PSII, stomatal conductance, Transpiration, Water use efficiency	Sobic.001G248300, Sobic.001G248500	Acylamino acid-peptidase-related, glutathione reductase	Chl, Chl	Tx430, Tx430
1_20	56058472	1	6	A recov, ΦPSII recov	QDMGR1.23, QGLFA1.10, QGLFA1.9, QSTCD1.25	Dry matter growth rate, Green leaf area, stomatal conductance	Sobic.001G286100	Inositol 1,3,4-trisphosphate 5/6-kinase family protein		Both
4_1	3797939–3800779	3	20	A recov, ΦPSII recov	QCHLF4.18, QDMGR4.9, QGYLD4.8, QTNGL4.1, QTNGL4.2	Chlorophyll fluorescence, Dry matter growth rate, Grain yield, Total no. of green leaves	Sobic.004G046200, Sobic.004G046500	Sulfotransferase 4A, Small GTP-binding protein	Chl	Tx642, Both

Table 2. Continued

GWAS					Overlapping QTL[a]		Promising candidate genes			
Region[b]	Physical interval[c]	No. of SNPs	No. of genes[d]	Traits	QTL ID	Traits	ID	Predicted function	Signal[e]	DE drought[f]
4_2	3813276–5677473	7	56	E recov, g_s recov, F_v/F_m' recov, ΦPSII recov	QCHLF4.18	Chlorophyll fluorescence	Sobic.004G047100	EPS15 homology domain 1	Chl/mt	TX642
					QDMGR4.9	Dry matter growth rate	Sobic.004G069850	Cyclase family protein	Chl	Tx642
					QGYLD4.8	Grain yield	Sobic.004G070000	Cyclase family protein		Both
					QTNGL4.1, QTNGL4.2	Total no of green leaves	Sobic.004G070200	RNA-metabolizing metallo-beta-lactamase		Both
4_7	62405510–62425357	2	23	E drought, E cum res, F_v/F_m' ratio DC, ΦPSII ratio DC	QCHLF4.16, CHLF4.17	Chlorophyll fluorescence	Sobic.004G281600	Mechanosensitive ion channel	Mt	Both
							Sobic.004G282000	Pentatricopeptide repeat prot	Chl	Both
							Sobic.004G282400	Rho GTPase activating prot		Both
7_3	60259969	2	14	g_s recov, F_v/F_m' recov	QTRSP7.1	Transpiration	Sobic.007G168000	Chlorophyllase 1		Both

Promising candidate genes were selected based on differential expression under drought conditions in a previous study, predicted peptide signal targeting to chloroplast or mitochondria, and predicted function.

[a] QTL physical coordinates and target traits were extracted from the Sorghum QTL Atlas (Mace et al., 2019) for the following 17 studies investigating drought stress response and/or photosynthesis-related traits in sorghum: Crasta et al., 1999; Haussman et al., 2002; Srinivas et al., 2009; Subudhi et al., 2000; Tao et al., 2000; Kapanigowda et al., 2014; Kebede et al., 2001; Fiedler et al., 2014, 2016; Ortiz et al., 2016; Phuong et al., 2013; Chopra et al., 2017; Rama Reddy et al., 2014; Sabadin et al., 2012; Sakhi et al., 2013; Sukumaran et al., 2016; Xu et al., 2000.

[b] Significantly associated genomic regions are labelled as chromosome#_region#.

[c] Physical position based on sorghum genome v.3.

[d] Total number of predicted genes within 55 kb of significant markers according to sorghum genome v.3.

[e] Predicted N-terminal transit peptide targeting protein to mitochondria or chloroplast, according to TargetP-2.0 (Almagro Armenteros et al., 2019).

[f] Indicates if differentially expressed under pre-flowering drought stress in Tx642, Tx430, or both lines, according to Varoquaux et al. (2019).

Table 3. Significant genome-wide associations that do not co-localize with any known QTL

| GWAS | | | | Traits | Candidate genes | | | |
Region[a]	Physical interval[b]	No. of SNPs	No. of genesc[b]		Most promising	Predicted function	Signal[d]	DE drought[e]
1_22	58204300–58204403	4	11	A recov, ΦPSII recov	Sobic.001G300201	HLH transcription factor		Tx430
					Sobic.001G300700	Expansin B		Tx642
1_23	58515970	1	8	A recov	Sobic.001G302300	Unknown function		both
2_3	58959838	1	7	E recov, g_s recov, E cum res, F_v'/F_m' recov	Sobic.002G199900	Unknown function	Chl	Both
					Sobic.002G200200	CAAX-Nterminal protease		Tx642
5_4	68758327-68758354	2	11	A recov, gs recov	Sobic.005G202600	Tropinone reductase		Tx430
5_5	71668462-71668533	3	20	E recov, g_s recov, F_v'/F_m' recov	Sobic.005G229000	SC35-like splicing factor 30		Tx642
					Sobic.005G229400	GRAS family TF		Tx642
					Sobic.005G229500	GRAS family TF		Tx642
					Sobic.005G229600	GRAS family TF		Tx642
					Sobic.005G229700	GRAS family TF		Tx642
					Sobic.005G229900	GRAS family TF		Tx430
					Sobic.005G230100	GRAS family TF		Tx642

Promising candidate genes were selected based on differential expression under drought conditions in a previous study, predicted peptide signal targeting to chloroplast or mitochondria, and predicted function.

[a] Significantly associated genomic regions are labeled as chromosome#_region#.

[b] Physical position based on sorghum genome v.3.

[c] Total number of predicted genes within 55 kb of significant markers according to sorghum genome v.3.

[d] Predicted N-terminal transit peptide targeting protein to mitochondria or chloroplast, according to TargetP-2.0 (Almagro Armenteros et al., 2019).

[e] Indicates if differentially expressed under pre-flowering drought stress in Tx642, Tx430, or both lines, according to Varoquaux et al. (2019).

localization with previously reported QTL for agronomic performance under drought or photosynthesis-related traits under abiotic stress, which provides an initial independent validation that could be subsequently reinforced with functional studies. Eight regions on chromosomes 1, 4, and 7 co-localized with QTL related to chlorophyll fluorescence, E, Φ_{PSII}, g_s, A, chlorophyll content, dry matter growth rate, green leaf area, number of green leaves, water-use efficiency, and grain yield under drought stress. All these regions were discovered due to variation observed during the recovery period, except one (region 4_7) that was correlated with parameters quantified during drought or across periods (Table 2; Fig. 3).

The number of predicted genes in each of these eight prioritized regions (Fig. 4) varied from six to 56, but only 22 were differentially expressed in either Tx642, Tx430, or both lines during pre-flowering drought stress according to Varoquaux *et al.* (2019). The presence of a predicted N-terminal peptide pre-sequence for the subcellular localization to mitochondria or chloroplasts was detected in 10 of these 22 most promising candidates for future studies and genetic manipulation (Table 2).

In region 1_9, two promising candidates are predicted to encode proteins targeted to the chloroplast (Table 2). *Sobic.001G248300* is homologous to acylamino acid–releasing enzymes (AAREs) (58% identity to *At4g14570*), which are involved in the turnover and destabilization of acetylated proteins, such as Rubisco, under oxidative conditions in Arabidopsis (Yamauchi *et al.*, 2003). Glutathione reductases are involved in scavenging reactive oxygen species (ROS) through the ascorbate–glutathione cycle and are essential to maintain efficient photosynthesis particularly under stress (Müller-Schüssele *et al.*, 2020). *Sobic.001G248500* is homologous to Arabidopsis *GR2* (*At3g54660*, 66% identity), which is essential in the plastid stroma (Marty *et al.*, 2019), protecting PSII from excess light and maintaining the repair of photodamaged PSII (Ding *et al.*, 2016).

One gene is singled out from regions 1_8, 1_20, and 7_3, considering the previously reported differential expression under drought, but none of them contains chloroplast or mitochondria targeting signals (Table 2). Endoplasmic reticulum-type Ca^{2+}-transporting ATPases (predicted function for *Sobic.001G103300*) are required and up-regulated to maintain low Ca^{2+} cytosolic levels by sequestering ions to intracellular compartments, which are used by plants to trigger signaling pathways in response to abiotic stress (Knight *et al.*, 1997; Aslam *et al.*, 2017). *Sobic.001G286100* is similar (84% identity) to an inositol 1,3,4-trisphosphate 5/6 kinase (ITPK). The overexpression of a rice ITPK homolog generated a drought- and salt-hypersensitive response, with a decrease in inositol trisphosphate and down-regulation of ROS-scavenging genes (Du *et al.*, 2011). Under abiotic stress, chlorophyll molecules are released from thylakoid membranes and should be degraded quickly to avoid damage induced by their photodynamic capacity (Takamiya *et al.*, 2000). Chlorophyllases catalyze this breakdown of chlorophyll but not as a consequence of senescence.

Sobic.007G168000 is predicted as a chlorophyllase-1, homolog of *At1g19670*, which has been associated with the degradation of chlorophyll, and whose silencing caused accumulation of hydrogen peroxide under high light conditions and induction of antioxidant mechanisms (Kariola *et al.*, 2005).

Three promising candidates were identified in region 4_7 (Table 2). *Sobic.004G281600* is predicted to encode a mitochondrial mechanosensitive ion channel protein with 54% identity to Arabidopsis *MSL1* (*At4g00290*). If the mitochondria membrane potential is too high, the ROS production and lipid peroxidation are increased. Ion transport mediated by *MSL1* reduced the mitochondrial membrane potential under stress, as demonstrated by the increased oxidation of the mitochondria glutathione pool in *MSL1* knockout mutants (Lee *et al.*, 2016). *Sobic.004G282000* contains a pentatricopeptide repeat (PPR) and the highest homology to several members of PPR-containing proteins in Arabidopsis that act in RNA editing which occurs in both chloroplasts and mitochondria (*At2g13600* and *At1g11290*). As an example, a mutation in *SLO2* (*At2g13600*) caused hypersensitivity to abscisic acid (ABA), accumulation of ROS, and increased drought tolerance (Zhu *et al.*, 2014), while inducing changes in RNA editing at seven sites of proteins belonging to complex I of the mitochondrial electron transport chain (Zhu *et al.*, 2012). Chloroplast PPR genes have also been associated with RNA editing and photosynthetic capacity, as demonstrated by the knockout mutation of *OsPPR16*, which edited *rpoB* RNA of the plastid-encoded RNA polymerase, affecting chlorophyll synthesis and normal chloroplast development (Huang *et al.*, 2020). *Sobic.004G282400* encodes a Rho GTPase-activating protein homologous to the product of *At3g11490* (62% identity), whose knockout mutants expressed an increased sensitivity to stress induced by oxygen deprivation.

Another region on chromosome 4 (4_2) harbors a homolog of *At3g20290* (*Sobic.004G047100*) which is predicted to encode an AtEHD1 protein required for endocytosis and membrane trafficking of recycling endosomes (Bar *et al.*, 2013). Altering the balance between exo- and endocytic protein trafficking, particularly of K^+ ion channels, affects adaptation to environmental clues (Bar *et al.*, 2013; Zhao *et al.*, 2017), as demonstrated by the defective stomatal movement caused by a reduction in endocytosis leading to dehydration tolerance (Larson *et al.*, 2017; Zhang *et al.*, 2019). Two cyclases in this region (*Sobic.004G069850* and *Sobic.004G070000*) had 64–79% identity to Arabidopsis cyclase genes *CYL1*, *CYL2*, and *CYL3*, a family that has been associated with the accumulation of ROS and response to multiple abiotic stresses (Qin *et al.*, 2015). *Sobic.004G070200* encodes a protein targeted to the chloroplast that is involved in rRNA and mRNA maturation (65% identity to *At5g63420*). Silencing of *At5g63420* caused chlorosis and revealed its role in the normal formation of thylakoid membranes (Chen *et al.*, 2015) and the reduction of RNA antisense–sense duplexes affecting chloroplast RNA quality (Hotto *et al.*, 2020) (Table 2).

An RNA helicase (*Sobic.001G126500*) was singled out in region 1_15, due to the known role of helicases in ribosome biogenesis and abiotic stress tolerance (Liu and Imai, 2018), particularly affecting photosynthesis and the antioxidant machinery (Tuteja *et al.*, 2013; Nawaz and Kang, 2019). A predicted chloroplast-targeted protein (*Sobic.001G128600*) with an unknown function is a homolog to the product of *At1g54520* (62% identity), which was identified as part of the chloroplast envelope and stroma–-lamella fraction, differentially phosphorylated in response to *STN8*. The transition from cyclic to linear electron flow upon illumination is mediated by *STN8* (Reiland *et al.*, 2011). *Sobic.001G129700* encodes a germin–like (oxalate oxidase) protein (77% identity to P15290 from wheat) that was differentially expressed in an osmotic stress study using sorghum cell cultures (Ashwin Ngara *et al.*, 2018). Tobacco plants overexpressing oxalate oxidase from wheat had a higher H_2O_2 concentration, higher expression of antioxidant enzyme genes, and increased tolerance to oxidative stress induced by high light (Hunt and Gray, 2009). Epidermal patterning factors (EPFs) are regulators of stomatal development, affecting density and spacing. *Sobic.001G140400* is a homolog to EPF-like2 (48% identity to NP_680774), and overexpression of EPFL genes leads to reduced stomatal density and increased drought tolerance in rice and Arabidopsis (Wan *et al.*, 2009; Caine *et al.*, 2019). Finally, pyruvate kinases, which catalyze the last step of glycolysis, are differentially regulated by drought in many tissues. *Sobic.001G140700* is a chloroplast-targeted pyruvate kinase, which could be responding to changes in oxygen levels due to stomatal closing, and compensanting for energy losses, as previously reported in barley (Janiak *et al.*, 2018) (Table 2).

New loci associated with photosynthetic response during the recovery period

Five LD regions on chromosomes 1, 2, and 5 were associated with gas exchange and/or chlorophyll fluorescence parameters and did not localize with previously reported QTL for agronomic performance under drought or photosynthesis-related traits (Table 3). All regions explained variation during the recovery period and harbored a total of 64 predicted genes. Twenty of these candidates were differentially expressed under drought (Varoquaux *et al.*, 2019) and represent the most promising targets for future functional validation and manipulation to improve drought tolerance.

On chromosome 1 (regions 1_22 and 1_23), *Sobic.001G300201* encodes a basic helix–loop–helix (bHLH) transcription factor with homology to *ZmPIF1* (GRMZM2G115960) (63% identity). Transgenic rice and Arabidopsis expressing *ZmPIF1* exhibited drought resistance due to a reduced stomatal conductance and transpiration mediated by ABA (Gao *et al.*, 2018). Expansins (EXPs), a predicted function of *Sobic.001G300700*, are cell wall proteins

involved in cell growth and reported to induce drought tolerance in wheat (Zhao *et al.*, 2011). Overexpression of wheat *EXPB23* led to transgenic tobacco plants that lost water more slowly, and maintain better cell structure and superior photosynthetic performance under drought stress (Li *et al.*, 2011). Similar results were obtained in sugarcane and potato (Chen *et al.*, 2019; Ashwin Narayan *et al.*, 2021). *Sobic.001G302300* encodes a protein of unknown function but with low homology to SNOWY COTYLEDON 3 (SCO3) protein in Arabidopsis (*At3g19570*; 28% identity). This gene that belongs to a large uncharacterized family unique to plants is required for normal chloroplast biogenesis and its mutation reduces chlorophyll accumulation, thylakoid formation, and photosynthesis (Albrecht *et al.*, 2010) (Table 3).

In region 2_3, *Sobic.002G199900* is predicted to encode a protein with homology to the plant peptide-containing tyrosine sulfation (PSY) family (Table 3). These small peptides are post-translationally modified and partially regulated at the transcriptional level, associated with the modulation of ABA responses to abiotic stress (Tost *et al.*, 2021). *Sobic.002G200200*, predicted to encode a chloroplast-targeted protein with homology to CaaX-like (59% identity to *At1g14270*), is a promising candidate because a CaaX-like endopeptidase (*SCO4* gene) was involved in the acclimation of chloroplasts and their photosystems to excesss light in Arabidopsis. *SCO4* mutants showed a decreased in linear electron transfer, reduced function of PSI, and increased NPQ (Albrecht-Borth *et al.*, 2013).

Out of the 13 genes localized in region 5_4, two were differentially expressed under drought conditions, but only *Sobic.005G202600* has a predicted function related to our traits (Table 3). It has homology to a senescence-associated protein 13 (SAG13) (74% identity to *At2g29350*), which is a small alcohol dehydrogenase/oxidoreductase that responds quickly and strongly to ABA treatments, not only in older leaves or as an indirect response to senescence (Weaver *et al.*, 1998).

The last newly associated region 5_5 harbored the largest number of genes, with 11 of them reported as differentially expressed in response to drought (Varoquaux *et al.*, 2019). *Sobic.005G229000* is one of the most promising candidates based on its homology to SC35-like splicing factor 30 (79% identity to *At3g55460*), which is an RNA-binding protein, part of the spliceosome that is responsive to drought stress (Marondedze *et al.*, 2020). Interestingly, a tandem of six GRAS-type transcription factors were localized in this region (Table 3). In Arabidopsis, this transcription factor family has been associated with numerous growth and development functions, having redundant roles (Lee *et al.*, 2008). In rice, *OsGRAS23* was located in a drought-resistant QTL, and, when overexpressed, plants showed drought resistance and tolerance to oxidative stress. Several antioxidation genes were also up-regulated in these transgenic plants (Xu *et al.*, 2015).

Concluding remarks

Our study aimed to characterize and exploit the sorghum natural variation in photosynthetic performance under optimal growing conditions, in response to drought and during the subsequent recovery to elucidate the genetic architecture of these important traits, and ultimately identify candidate genes for genetic improvement, engineering, or editing. The response to abiotic stress is complex in nature and involves the expression of multiple genes with small effects. To address this challenge, the GWAS presented herein was conducted using a large number of accessions and was complemented by comparative studies with previously reported QTL of related traits, public RNAseq data, and prediction of organelle targeting peptide signals. The most important discoveries are: (i) there is large natural variation in gas exchange and chlorophyll fluorescence traits in response to non-stress, drought, and recovery conditions; (ii) stomatal control was the main factor explaining reductions in gas exchange under drought and recovery treatments; (iii) sorghum lines presented a large *A:E* range under optimal growing conditions but minimal variation under drought and recovery; (iv) the majority of SNP–trait associations corresponded to the recovery treatment, revealing the importance of exploiting post-stress adaptation mechanisms; (v) 39 significant SNPs are co-localized with previously reported QTL for stay-green in sorghum even though drought stress was imposed during pre-flowering; and (vi) 22 promising candidate genes were identified based on multiple layers of selection and homology to genes with functions related to photosynthesis and photoprotection. Finally, our results represent a valuable resource to select genotypes with enhanced tolerance to drought stress. The exploration of syntenic regions with other species such as maize, wheat, and rice could also support breeding efforts to enhance carbon fixation capacity in other commercially important crops.

Supplementary data

The following supplementary data are available at *JXB* online.

Fig. S1. Photosynthesis (*A*) as a function of stomatal conductance (*g*$_s$) in sorghum in control (30% VWC), drought (15 % VWC), and recovery periods (30% VWC).

Fig. S2. Photosynthesis (*A*) as a function of effective quantum yield of PSII (ΦPSII) in sorghum in control (30% VWC), drought (15 % VWC), and recovery periods (30% VWC).

Fig. S3. Genome-wide association study results for *A* in three soil water content treatments and in cumulative response, drought/control ratio, and drought/recovery ratio using 324 diverse sorghum accessions.

Fig. S4. Genome-wide association study results for *E* in three soil water content treatments and in cumulative response, drought/control ratio, and drought/recovery ratio using 324 diverse sorghum accessions.

Fig. S5. Genome-wide association study results for *g*$_s$ in three soil water content treatments and in cumulative response, drought/control ratio, and drought/recovery ratio using 324 diverse sorghum accessions.

Fig. S6. Genome-wide association study results for F_v/F_m in three soil water content treatments and in cumulative response, drought/control ratio, and drought/recovery ratio using 324 diverse sorghum accessions.

Fig. S7. Genome-wide association study results for F_v'/F_m' in three soil water content treatments and in cumulative response, drought/control ratio, and drought/recovery ratio using 324 diverse sorghum accessions.

Fig. S8. Genome-wide association study results for Φ_{PSII} in three soil water content treatments and in cumulative response, drough/control ratio, and drought/recovery ratio using 324 diverse sorghum accessions.

Fig. S9. Genome-wide association study results for qP in three soil water content treatments and in cumulative response, drought/control ratio, and drought/recovery using 324 diverse sorghum accessions.

Fig. S10. Genome-wide association study results for *A:E* ratio in three soil water content treatments using 324 diverse sorghum accessions.

Table S1. Soil water content (VWC) of 324 accessions averaged across the last 3 d of drought treatment.

Table S2. Phenotypic correlations between photosynthesis and chlorophyll fluorescence traits based on BLUPs in the control period.

Table S3. Phenotypic correlations between photosynthetic and chlorophyll fluorescence traits based on BLUPs in the drought period.

Table S4. Phenotypic correlations between photosynthetic and chlorophyll fluorescence traits based on BLUPs in the recovery period.

Table S5. ANOVA of photosynthesis and chlorophyll fluorescence traits in control, drought, and recovery periods.

Table S6. Summary of GWAs results for gas exchange and chlorophyll fluorescence traits in control, drought, and recovery periods, derived variables cumulative response, and drought/recovery ratio.

Table S7. Complete list of sorghum genes localized ±55 kb of significant SNPs.

Table S8. Summary of associated regions co-localizing with previously published QTL for drought stress response and/or photosynthesis-related traits.

Table S9. Subset of associated LD regions for both gas exchange and chlorophyll fluorescence traits co-localized with QTL for drought response or photosynthesis-related traits.

Acknowledgements

Author contributions

MGSF and DO: designed the experiments and analyzed the data; DO: collected phenotypic data; MGSF and DO: contributed to writing and editing of the manuscript; MGSF: conceived the research idea and directed the project.

Conflict of interest

The authors declare that they have no conflict of interest.

Data availability

Genotypic data utilized for GWAS are publicly available at https://www.morrislab.org/data. The phenotypic data supporting findings of this study are available from the corresponding author, Maria G. Salas-Fernandez, upon request.

References

Albrecht V, Simková K, Carrie C, Delannoy E, Giraud E, Whelan J, Small ID, Apel K, Badger MR, Pogson BJ. 2010. The cytoskeleton and the peroxisomal-targeted snowy cotyledon3 protein are required for chloroplast development in Arabidopsis. The Plant Cell **22**, 3423–3438.

Albrecht-Borth V, Kauss D, Fan D, et al. 2013. A novel proteinase, SNOWY COTYLEDON4, is required for photosynthetic acclimation to higher light intensities in Arabidopsis. Plant Physiology **163**, 732–745.

Almagro Armenteros JJ, Salvatore M, Winther O, Emanuelsson O, von Heijne G, Elofsson A, Nielsen H. 2019. Detecting sequence signals in targeting peptides using deep learning. Life Science Alliance **2**, e201900429.

Ashwin Narayan JA, Chakravarthi M, Nerkar G, et al. 2021. Overexpression of expansin EaEXPA1, a cell wall loosening protein enhances drought tolerance in sugarcane. Industrial Crops and Products **159**, 113035.

Aslam R, Williams LE, Bhatti MF, Virk N. 2017. Genome-wide analysis of wheat calcium ATPases and potential role of selected ACAs and ECAs in calcium stress. BMC Plant Biology **17**, 174.

Balota M, Payne WA, Rooney W, Rosenow D. 2008. Gas exchange and transpiration ratio in sorghum. Crop Science **48**, 2361–2371.

Bar M, Leibman M, Schuster S, Pitzhadza H, Avni A. 2013. EHD1 functions in endosomal recycling and confers salt tolerance. PLoS One **8**, e54533.

Björkman O, Demmig B. 1987. Photon yield of O_2 evolution and chlorophyll fluorescence characteristics at 77 K among vascular plants of diverse origins. Planta **170**, 489–504.

Blum A. 2011. Drought resistance—is it really a complex trait? Functional Plant Biology **38**, 753–757.

Borrell AK, Hammer GL, Henzell RG. 2000. Does maintaining green leaf area in sorghum improve yield under drought? II. Dry matter production and yield. Crop Science **40**, 1037–1048.

Burke JJ, Chen J, Burow G, Mechref Y, Rosenow D, Payton P, Xin Z, Hayes CM. 2013. Leaf dhurrin content is a quantitative measure of the level of pre- and postflowering drought tolerance in sorghum. Crop Science **53**, 1056–1065.

Caine RS, Yin X, Sloan J, et al. 2019. Rice with reduced stomatal density conserves water and has improved drought tolerance under future climate conditions. New Phytologist **221**, 371–384.

Casa AM, Pressoir G, Brown PJ, Mitchell SE, Rooney WL, Tuinstra MR, Franks CD, Kresovich S. 2008. Community resources and strategies for association mapping in sorghum. Crop Science **48**, 30–40.

Chaves MM, Flexas J, Pinheiro C. 2009. Photosynthesis under drought and salt stress: regulation mechanisms from whole plant to cell. Annals of Botany **103**, 551–560.

Chen H, Zou W, Zhao J. 2015. Ribonuclease J is required for chloroplast and embryo development in Arabidopsis. Journal of Experimental Botany **66**, 2079–2091.

Chen Y, Zhang B, Li C, Lei C, Kong C, et al. 2019. A comprehensive expression analysis of the expansin gene family in potato (*Solanum tuberosum*) discloses stress-responsive expansin-like B genes for drought and heat tolerances. PLoS One **14**, e0219837.

Chopra R, Burow G, Burke JJ, et al. 2017. Genome-wide association analysis of seedling traits in diverse Sorghum germplasm under thermal stress. BMC Plant Biology **17**, 12.

Collins NC, Tardieu F, Tuberosa R. 2008. Quantitative trait loci and crop performance under abiotic stress: where do we stand? Plant Physiology **147**, 469–486.

Cornic G. 2017. Drought stress inhibits photosynthesis by decreasing stomatal aperture—not by affecting ATP synthesis. Trends in Plant Science **5**, 187–188.

Cousins AB, Adam NR, Wall GW, Kimball BA, Pinter PJ, Ottman MJ, Leavitt SW, Webber AN. 2002. Photosystem II energy use, non-photochemical quenching and the xanthophyll cycle in *Sorghum bicolor* grown under drought and free-air CO_2 enrichment (FACE) conditions. Plant, Cell & Environment **25**, 1551–1559.

Crasta OR, Xu WW, Rosenow DT, Mullet J, Nguyen HT. 1999. Mapping of post-flowering drought resistance traits in grain sorghum: association between QTLs influencing premature senescence and maturity. Molecular and General Genetics **262**, 579–588.

Demmig-Adams B, Winter K, Krüger A, Czygan FC. 1989. Zeaxanthin synthesis, energy dissipation, and photoprotection of photosystem II at chilling temperatures. Plant Physiology **90**, 894–898.

Ding S, Jiang R, Lu Q, Wen X, Lu C. 2016. Glutathione reductase 2 maintains the function of photosystem II in Arabidopsis under excess light. Biochimica et Biophysica Acta **1857**, 665–677.

Du H, Liu L, You L, Yang M, He Y, Li X, Xiong L. 2011. Characterization of an inositol 1,3,4-trisphosphate 5/6-kinase gene that is essential for drought and salt stress responses in rice. Plant Molecular Biology **77**, 547–563.

Elshire RJ, Glaubitz JC, Sun Q, Poland JA, Kawamoto K, Buckler ES, Mitchell SE. 2011. A robust, simple genotyping-by-sequencing (GBS) approach for high diversity species. PLoS One **6**, e19379.

FAO. 2016. Climate change and food security: risks and responses. Rome: Food and Agriculture Organization.

Fiedler K, Bekele WA, Duensing R, Gründig S, Snowdon R, Stützel H, Zacharias A, Uptmoor R. 2014. Genetic dissection of temperature-dependent sorghum growth during juvenile development. Theoretical and Applied Genetics **127**, 1935–1948.

Fiedler K, Bekele W, Matschegewski C, Snowdon R, Wieckhorst S, Zacharias A, Uptmoor R. 2016. Cold tolerance during juvenile development in sorghum: a comparative analysis by genomewide association and linkage mapping. Plant Breeding **135**, 598–606.

Finkel E. 2009. Imaging: With 'Phenomics', plant scientists hope to shift breeding into overdrive. Science **325**, 380–381.

Flood PJ, Harbinson J, Aarts MGM. 2011. Natural genetic variation in plant photosynthesis. Trends in Plant Science **16**, 327–335.

Fracheboud Y, Haldimann P, Leipner J, Stamp P. 1999. Chlorophyll fluorescence as a selection tool for cold tolerance of photosynthesis in maize (*Zea mays* L.). Journal of Experimental Botany **50**, 1533–1540.

Fracheboud Y, Ribaut JM, Vargas M, Messmer R, Stamp P. 2002. Identification of quantitative trait loci for cold-tolerance of photosynthesis in maize (*Zea mays* L.). Journal of Experimental Botany **53**, 1967–1977.

Gao Y, Wu M, Zhang M, *et al*. 2018. A maize phytochrome-interacting factors protein ZmPIF1 enhances drought tolerance by inducing stomatal closure and improves grain yield in *Oryza sativa*. Plant Biotechnology Journal **16**, 1375–1387.

Genty B, Briantais JM, Baker NR. 1989. The relationship between the quantum yield of photosynthetic electron transport and quenching of chlorophyll fluorescence. Biochimica et Biophysica Actas **990**, 87–92.

Granier C, Aguirrezabal L, Chenu K, *et al*. 2006. PHENOPSIS, an automated platform for reproducible phenotyping of plant responses to soil water deficit in *Arabidopsis thaliana* permitted the identification of an accession with low sensitivity to soil water deficit. New Phytologist **169**, 623–635.

Gu J, Yin X, Struik PC, Stomph TJ, Wang H. 2012. Using chromosome introgression lines to map quantitative trait loci for photosynthesis parameters in rice (*Oryza sativa* L.) leaves under drought and well-watered field conditions. Journal of Experimental Botany **63**, 455–469.

Guo P, Baum M, Varshney R, Graner A, Grando S, Ceccarelli S. 2008. QTLs for chlorophyll and chlorophyll fluorescence parameters in barley under post-flowering drought. Euphytica **163**, 203–214.

Hao D, Chao M, Yin Z, Yu D. 2012. Genome-wide association analysis detecting significant single nucleotide polymorphisms for chlorophyll and chlorophyll fluorescence parameters in soybean (*Glycine max*) landraces. Euphytica **186**, 919–931.

Hardy OJ, Vekemans X. 2002. SPAGeDi: a versatile computer program to analyse spatial genetic structure at the individual or population levels. Molecular Ecology Notes **2**, 618–620.

Haussmann BIG, Hess DE, Seetharama N, Welz HG, Geiger HH. 2002. Construction of a combined sorghum linkage map from two recombinant inbred populations using AFLP, SSR, RFLP, and RAPD markers, and comparison with other sorghum maps. Theoretical and Applied Genetics **105**, 629–637.

Hervé D, Fabre F, Flores Berrios E, Leroux N, Al Chaarani G, Planchon C, Sarrafi A, Gentzbittel L. 2001. QTL analysis of photosynthesis and water status traits in sunflower (*Helianthus annuus* L.) under greenhouse conditions. Journal of Experimental Botany **52**, 1857–1864.

Hotto AM, Stern DB, Schuster G. 2020. Plant ribonuclease J: an essential player in maintaining chloroplast RNA quality control for gene expression. Plants **9**, 334.

Huang W, Zhang Y, Shen L, *et al*. 2020. Accumulation of the RNA polymerase subunit RpoB depends on RNA editing by OsPPR16 and affects chloroplast development during early leaf development in rice. New Phytologist **228**, 1401–1416.

Hund A, Frascaroli E, Leipner J, Jompuk C, Stamp P, Fracheboud Y. 2005. Cold tolerance of the photosynthetic apparatus: pleiotropic relationship between photosynthetic performance and specific leaf area of maize seedlings. Molecular Breeding **16**, 321–331.

Hunt L, Gray JE. 2009. The signaling peptide EPF2 controls asymmetric cell divisions during stomatal development. Current Biology **19**, 864–869.

Janiak A, Kwasniewski M, Sowa M, Gajek K, Żmuda K, Kościelniak J, Szarejko I. 2018. No time to waste: transcriptome study reveals that drought tolerance in barley may be attributed to stressed-like expression patterns that exist before the occurrence of stress. Frontiers in Plant Science **8**, 2212.

Junker A, Muraya MM, Weigelt-Fischer K, Arana-Ceballos F, Klukas C, Melchinger AE, Meyer RC, Riewe D, Altmann T. 2015. Optimizing experimental procedures for quantitative evaluation of crop plant performance in high throughput phenotyping systems. Frontiers in Plant Science **5**, 770.

Kapanigowda MH, Payne WA, Rooney WL, Mullet JE, Balota M. 2014. Quantitative trait locus mapping of the transpiration ratio related to preflowering drought tolerance in sorghum (*Sorghum bicolor*). Functional Plant Biology **41**, 1049–1065.

Kariola T, Brader G, Li J, Palva ET. 2005. Chlorophyllase 1, a damage control enzyme, affects the balance between defense pathways in plants. The Plant Cell **17**, 282–294.

Kebede H, Subudhi PK, Rosenow DT, Nguyen HT. 2001. Quantitative trait loci influencing drought tolerance in grain sorghum (*Sorghum bicolor* L. Moench). Theorerical and Applied Genetics **103**, 266–276.

Kiani SP, Maury P, Sarrafi A, Grieu P. 2008. QTL analysis of chlorophyll fluorescence parameters in sunflower (*Helianthus annuus* L.) under well-watered and water-stressed conditions. Plant Science **175**, 565–573.

Kidambi S, Krieg D, Nguen H. 1990a. Parental influences on gas exchange rates in grain sorghum. Euphytica **50**, 139–146.

Kidambi SP, Krieg DR, Rosenow DT. 1990b. Genetic variation for gas exchange rates in grain sorghum. Plant Physiology **92**, 1211–1214.

Knight H, Trewavas AJ, Knight MR. 1997. Calcium signalling in *Arabidopsis thaliana* responding to drought and salinity. The Plant Journal **12**, 1067–1078.

Kościelniak J, Janowiak F, Kurczych Z. 2005. Increase in photosynthesis of maize hybrids (*Zea mays* L.) at suboptimal temperature (15 °C) by selection of parental lines on the basis of chlorophyll a fluorescence measurements. Photosynthetica **43**, 125–134.

Larson ER, Van Zelm E, Roux C, Marion-Poll A, Blatt MR. 2017. Clathrin heavy chain subunits coordinate endo- and exocytic traffic and affect stomatal movement. Plant Physiology **175**, 708–720.

Lawlor DW. 2002. Limitation to photosynthesis in water-stressed leaves: stomata vs. metabolism and the role of ATP. Annals of Botany **89**, 871–885.

Lee MH, Kim B, Song SK, *et al*. 2008. Large-scale analysis of the GRAS gene family in *Arabidopsis thaliana*. Plant Molecular Biology **67**, 659–670.

Lee CP, Maksaev G, Jensen GS, Murcha MW, Wilson ME, Fricker M, Hell R, Haswell ES, Millar AH, Sweetlove LJ. 2016. MSL1 is a mechanosensitive ion channel that dissipates mitochondrial membrane potential and maintains redox homeostasis in mitochondria during abiotic stress. The Plant Journal **88**, 809–825.

Li F, Xing S, Guo Q, Zhao M, Zhang J, Gao Q, Wang G, Wang W. 2011. Drought tolerance through over-expression of the expansin gene TaEXPB23 in transgenic tobacco. Journal of Plant Physiology **168**, 960–966.

Li Y, Ye W, Wang M, Yan X. 2009. Climate change and drought: a risk assessment of crop-yield impacts. Climate Research **39**, 31–46.

Liu Y, Imai R. 2018. Function of plant DExD/H-Box RNA helicases associated with ribosomal RNA biogenesis. Frontiers in Plant Science **9**, 125.

Long SP. 1999. Ecology of C$_4$ photosynthesis. Environmental responses. In: Monson RK, Sage RF, eds. C$_4$ plant biology. San Diego: Academic Press, 215–249.

Long SP, Zhu XG, Naidu SL, Ort DR. 2006. Can improvement in photosynthesis increase crop yields? Plant, Cell & Environment **29**, 315–330.

Mace E, Innes D, Hunt C, Wang XM, Tao YF, Baxter J, Hassall M, Hathorn A, Jordan D. 2019. The Sorghum QTL Atlas: a powerful tool for trait dissection, comparative genomics and crop improvement. Theoretical and Applied Genetics **132**, 751–766.

Mantilla Perez MB, Zhao J, Yin Y, Hu J, Salas Fernandez MG. 2014. Association mapping of brassinosteroid candidate genes and plant architecture in a diverse panel of *Sorghum bicolor*. Theoretical and Applied Genetics **127**, 2645–2662.

Marondedze C, Thomas L, Lilley KS, Gehring C. 2020. Drought stress causes specific changes to the spliceosome and stress granule components. Frontiers in Molecular Biosciences **6**, 163.

Marty L, Bausewein D, Müller C, *et al*. 2019. Arabidopsis glutathione reductase 2 is indispensable in plastids, while mitochondrial glutathione is safeguarded by additional reduction and transport systems. New Phytologist **224**, 1569–1584.

Maxwell K, Johnson GN. 2000. Chlorophyll fluorescence—a practical guide. Journal of Experimental Botany **51**, 659–668.

McCormick RF, Truong SK, Sreedasyam A, *et al*. 2018. The *Sorghum bicolor* reference genome: improved assembly, gene annotations, a transcriptome atlas, and signatures of genome organization. The Plant Journal **93**, 338–354.

Mcdonald AJS, Davies WJ. 1996. Keeping in touch: responses of the whole plant to deficits in water and nitrogen supply. Advances in Botanical Research **22**, 229–300.

Morris GP, Ramu P, Deshpande SP, et al. 2013. Population genomic and genome-wide association studies of agroclimatic traits in sorghum. Proceedings of the National Academy of Sciences, USA **110**, 453–458.

Müller-Schüssele SJ, Wang R, Gütle DD, et al. 2020. Chloroplasts require glutathione reductase to balance reactive oxygen species and maintain efficient photosynthesis. The Plant Journal **103**, 1140–1154.

Nawaz G, Kang H. 2019. Rice OsRH58, a chloroplast DEAD-box RNA helicase, improves salt or drought stress tolerance in Arabidopsis by affecting chloroplast translation. BMC Plant Biology **19**, 17.

Netondo GW, Onyango JC, Beck E. 2004. Sorghum and salinity: II. Gas exchange and chlorophyll fluorescence of sorghum under salt stress. Crop Science **44**, 806–811.

Noodén LD, John I, Guiamét JJ. 1997. Senescence mechanisms. Physiologia Plantarum **101**, 746–753.

Ortiz D, Hu J, Salas Fernandez MG. 2017. Genetic architecture of photosynthesis in *Sorghum bicolor* under non-stress and cold stress conditions. Journal of Experimental Botany **68**, 4545–4557.

Ortiz D, Litvin AG, Salas Fernandez MG. 2018. A cost-effective and customizable automated irrigation system for precise high-throughput phenotyping in drought stress studies. PLoS One **13**, e0198546.

Peng S, Krieg D, Girma F. 1991. Leaf photosynthetic rate is correlated with biomass and grain production in grain sorghum lines. Photosynthesis Research **28**, 1–7.

Phuong N, Stützel H, Uptmoor R. 2013. Quantitative trait loci associated to agronomic traits and yield components in a *Sorghum bicolor* L. Moench RIL population cultivated under pre-flowering drought and well-watered conditions. Agricultural Sciences **4**, 781–791.

Pritchard JK, Stephens M, Rosenberg NA, Donnelly P. 2000. Association mapping in structured populations. American Journal of Human Genetics **67**, 170–181.

Qin Y, Shen X, Wang N, Ding X. 2015. Characterization of a novel cyclase-like gene family involved in controlling stress tolerance in rice. Journal of Plant Physiology **181**, 30–41.

Rama Reddy NR, Ragimasalawada M, Sabbavarapu MM, et al. 2014. Detection and validation of stay-green QTL in post-rainy sorghum involving widely adapted cultivar, M35-1 and a popular stay-green genotype B35. BMC Genomics **15**, 909.

Reiland S, Finazzi G, Endler A, et al. 2011. Comparative phosphoproteome profiling reveals a function of the STN8 kinase in fine-tuning of cyclic electron flow (CEF). Proceedings of the National Academy of Sciences, USA **108**, 12955–12960.

Ruban AV, Johnson MP, Duffy CDP. 2012. The photoprotective molecular switch in the photosystem II antenna. Biochimica et Biophysica Acta **1817**, 167–181.

Sabadin PK, Malosetti M, Boer MP, et al. 2012. Studying the genetic basis of drought tolerance in sorghum by managed stress trials and adjustments for phenological and plant height differences. Theoretical and Applied Genetics **124**, 1389–1402.

Sakhi S, Shehzad T, Rehman S, Okiuno K. 2013. Mapping the QTLs underlying drought stress at developmental stage of sorghum (*Sorghum bicolor* (L.) Moench) by association analysis. Euphytica **193**, 433–450.

Salas Fernandez MG, Strand K, Hamblin MT, Westgate M, Heaton E, Kresovich S. 2015. Genetic analysis and phenotypic characterization of leaf photosynthetic capacity in a sorghum (*Sorghum* spp.) diversity panel. Genetic Resources and Crop Evolution **62**, 939–950.

Sanchez AC, Subudhi PK, Rosenow DT, Nguyen HT. 2002. Mapping QTLs associated with drought resistance in sorghum (*Sorghum bicolor* L. Moench). Plant Molecular Biology **48**, 713–726.

Sankarapandian R, Audilakshmi S, Sharma V, Ganesamurthy K, Talwar HS, Patil JV. 2013. Effect of morpho-physiological traits on grain yield of sorghum grown under stress at different growth stages, and stability analysis. Journal of Agricultural Science **151**, 630–647.

Srinivas G, Satish K, Madhusudhana R, Nagaraja Reddy R, Murali Mohan S, Seetharama N. 2009. Identification of quantitative trait loci for agronomically important traits and their association with genic-microsatellite markers in sorghum. Theoretical and Applied Genetics **118**, 1439–1454.

Storey JD, Tibshirani R. 2003. Statistical significance for genomewide studies. Proceedings of the National Academy of Sciences, USA **100**, 9440–9445.

Strigens A, Freitag NM, Gilbert X, Grieder C, Riedelsheimer C, Schrag TA, Messmer R, Melchinger AE. 2013. Association mapping for chilling tolerance in elite flint and dent maize inbred lines evaluated in growth chamber and field experiments. Plant, Cell & Environment **36**, 1871–1887.

Subudhi PK, Rosenow DT, Nguyen HT. 2000. Quantitative trait loci for the stay green trait in sorghum (*Sorghum bicolor* L. Moench): consistency across genetic backgrounds and environments. Theoretical and Applied Genetics **101**, 733–741.

Sukumaran S, Li X, Li X, et al. 2016. QTL mapping for grain yield, flowering time, and stay-green traits in sorghum with genotyping-by-sequencing markers. Crop Science **56**, 1429–1442.

Sukumaran S, Xiang W, Bean SR, Pedersen JF, Kresovich S, Tuinstra MR, Tesso TT, Hamblin MT, Yu J. 2012. Association mapping for grain quality in a diverse sorghum collection. Plant Genome **5**, 126–135.

Takamiya KI, Tsuchiya T, Ohta H. 2000. Degradation pathway(s) of chlorophyll: what has gene cloning revealed? Trends in Plant Science **5**, 426–431.

Tao YZ, Henzell RG, Jordan DR, Butler DG, Kelly AM, McIntyre CL. 2000. Identification of genomic regions associated with stay green in sorghum by testing RILs in multiple environments. Theoretical and Applied Genetics **100**, 1225–1232.

Tari I, Laskay G, Takács Z, Poór P. 2013. Response of Sorghum to abiotic stresses: a review. Journal of Agronomy and Crop Science **199**, 264–274.

Taylor SH, Hulme SP, Rees M, Ripley BS, Woodward FI, Osborne CP. 2010. Ecophysiological traits in C$_3$ and C4 grasses: a phylogenetically controlled screening experiment. New Phytologist **185**, 780–791.

Tost AS, Kristensen A, Olsen LI, Axelsen KB, Fuglsang AT. 2021. The PSY peptide family—expression, modification and physiological implications. Genes **12**, 218.

Tuteja N, Sahoo RK, Garg B, Tuteja R. 2013. OsSUV3 dual helicase functions in salinity stress tolerance by maintaining photosynthesis and antioxidant machinery in rice (*Oryza sativa* L. cv. IR64). The Plant Journal **76**, 115–127.

van Rooijen R, Aarts MGM, Harbinson J. 2015. Natural genetic variation for acclimation of photosynthetic light use efficiency to growth irradiance in Arabidopsis. Plant Physiology **167**, 1412–1429.

Varoquaux N, Cole B, Gao C, et al. 2019. Transcriptomic analysis of field-droughted sorghum from seedling to maturity reveals biotic and metabolic responses. Proceedings of the National Academy of Sciences, USA **116**, 27124–27132.

Wan X, Tan J, Lu S, Lin C, Hu Y, Guo Z. 2009. Increased tolerance to oxidative stress in transgenic tobacco expressing a wheat oxalate oxidase gene via induction of antioxidant enzymes is mediated by H$_2$O$_2$. Physiologia Plantarum **136**, 30–44.

Weaver LM, Gan S, Quirino B, Amasino RM. 1998. A comparison of the expression patterns of several senescence-associated genes in response to stress and hormone treatment. Plant Molecular Biology **37**, 455–469.

Xin Z, Aiken R, Burke J. 2009. Genetic diversity of transpiration efficiency in sorghum. Field Crops Research **111**, 74–80.

Xu K, Chen S, Li T, Ma X, Liang X, Ding X, Liu H, Luo L. 2015. OsGRAS23, a rice GRAS transcription factor gene, is involved in drought stress response through regulating expression of stress-responsive genes. BMC Plant Biology **15**, 141.

Xu W, Subudhi PK, Crasta OR, Rosenow DT, Mullet JE, Nguyen HT. 2000. Molecular mapping of QTLs conferring stay-green in grain sorghum (*Sorghum bicolor* L. Moench). Genome **43**, 461–469.

Yamauchi Y, Ejiri Y, Toyoda Y, Tanaka K. 2003. Identification and biochemical characterization of plant acylamino acid-releasing enzyme. Journal of Biochemistry **134**, 251–257.

Zegada-Lizarazu W, Monti A. 2013. Photosynthetic response of sweet sorghum to drought and re-watering at different growth stages. Physiologia Plantarum **149**, 56–66.

Zhang L, Xing J, Lin J. 2019. At the intersection of exocytosis and endocytosis in plants. New Phytologist **224**, 1479–1489.

Zhang Z, Ersoz E, Lai CQ, *et al*. 2010. Mixed linear model approach adapted for genome-wide association studies. Nature Genetics **42**, 355–360.

Zhao J, Mantilla Perez MB, Hu J, Salas Fernandez MG. 2016. Genome-wide association study for nine plant architecture traits in sorghum. The Plant Genome **9**, doi: 10.3835/plantgenome2015.06.0044.

Zhao MR, Li F, Fang Y, Gao Q, Wang W. 2011. Expansin-regulated cell elongation is involved in the drought tolerance in wheat. Protoplasma **248**, 313–323.

Zhao P, Wang L, Zhao X, Chen G, Ma XF. 2017. A comparative transcriptomic analysis reveals the core genetic components of salt and osmotic stress responses in *Braya humilis*. PLoS One **12**, e0183778.

Zhu Q, Dugardeyn J, Zhang C, *et al*. 2012. SLO2, a mitochondrial pentatricopeptide repeat protein affecting several RNA editing sites, is required for energy metabolism. The Plant Journal **71**, 836–849.

Zhu Q, Dugardeyn J, Zhang Z, *et al*. 2014. The *Arabidopsis thaliana* RNA editing factor SLO2, which affects mitochondrial electron transport chain, participates in multiple stress and hormone responses. Molecular Plant **7**, 290–310.